View metadata, citation and similar papers at core.ac.uk

brought to you by CORE

provided by NASA Technical Reports Server

N O T I C E

THIS DOCUMENT HAS BEEN REPRODUCED FROM MICROFICHE. ALTHOUGH IT IS RECOGNIZED THAT CERTAIN PORTIONS ARE ILLEGIBLE, IT IS BEING RELEASED IN THE INTEREST OF MAKING AVAILABLE AS MUCH INFORMATION AS POSSIBLE

POSSIBLE ISOTOPIC FRACTIONATION EFFECTS IN SPUTTERED MINERALS*

P. K. HAFF, C. C. WATSON, and T. A. TOMBRELLO

W. K. Kellogg Radiation Laboratory

California Institute of Technology, Pasadena, California 91125

MAR 1981
RECEIVED
NASA STI FACILITY
ACCESS DEPT.

*Supported in part by the National Aeronautics and Space Administration [NGR-05-002-333] and by the National Science Foundation [PHY79-23638].

(NASA-CR-164042) POSSIBLE ISOTOPIC FRACTIONATION EFFECTS IN SPUTTERED MINERALS (California Inst. of Tech.) 36 p HC A03/MF A01 CSCL 07D

N81-19246

Unclas

G3/25 18093

ABSTRACT

We discuss in detail a model which makes definite predictions for the fractionation of isotopes in sputtered material. The fractionation patterns can be non-linear, and the pattern for a particular set of isotopes depends on the chemical matrix within which those isotopes are contained. Calculations are presented for all non-monoisotopic elements contained in the minerals perovskite, anorthite, ackermanite, enstatite, and troilite. All isotopes are fractionated at the level of approximately 4-6 $^{o}/oo$ per atomic mass unit. O is always positively fractionated (heavier isotopes sputtered preferentially), and heavier elements are generally negatively fractionated (lighter isotopes sputtered preferentially). The value of $\delta(^{18}O:^{16}O)$ is always less by about 1.8 $^{o}/oo$ than a linear extrapolation based upon the calculated $\delta(^{17}O:^{16}O)$ value would suggest. The phenomenon of both negative and positive fractionation patterns from a single target mineral can be used to make an experimental test of the proposed model.

Recent experiments [Russell et al., 1980] and theoretical models [Watson and Haff, 1980; Watson, 1980] have addressed the question of isotopic fractionation of surfaces which have been exposed to fluxes of low-energy (keV) ions. Earlier work has tended to center mainly on chemical composition changes produced by ion bombardment [Liau et al., 1977] since several convenient techniques (e.g., Rutherford backscattering) exist to analyze the near-surface composition as a function of depth. Theoretical studies of these processes, e.g., by Haff and Switkowski [1976], are always faced with the necessity of having to prescribe quantitatively the differences in chemical binding energies between atomic species in order to predict the degree of chemical fractionation. In experiments involving ion sputtering of isotopic components of a single element, the experimenter is faced with the complexities imposed by the small size of the expected effects, but the theoretical analysis of the sputtering process and the determination of relative sputtering yields for a given suite of isotopes is made correspondingly easier.

Based upon an original motivation to construct a sputtering theory of binary and more complicated materials, which could be tested against experiment, Watson [1980] and Watson and Haff [1980] developed a model which described the sharing of recoil energy amongst the components of a given target. The results of the investigation indicated that little fractionation was likely to occur if fractionation effects were due entirely to differences in the bulk recoil fluxes of constituent target atoms. The calculated fractionation, $\delta_{44,40}$, due to non-stoichometries in the internal fluxes alone was only $\sim -1\,^{o}/oo$ (parts per thousand) for ^{44}Ca with respect to ^{40}Ca in a mineral target. We here define

$$\delta_{1,2} \equiv \frac{S_1/n_1}{S_2/n_2} - 1 \qquad (1)$$

where S_i is the number of target atoms of type i sputtered per incident projectile, and n_i is the abundance of atoms of type i at the surface of the unsputtered target. Thus we compare the composition of the sputtered material to the undisturbed target composition. However, by making the critical assumption that the atoms found in the extreme outer layer cannot participate in the collision cascade on an equal footing with the internally recoiling atoms, Watson [1980]* arrived at an expression for the isotopic fractionation expected in the material sputtered by the collisional-recoil process from a surface containing isotopes of species k and ℓ,

$$\delta_{k,\ell} = \frac{\bar{\gamma}_k}{\bar{\gamma}_\ell} - 1 , \tag{2}$$

where

$$\bar{\gamma}_k \equiv \frac{\sum_i n_i \sigma_{ik} \gamma_{ik}}{\sum_i n_i \sigma_{ik}} - 1 , \tag{3}$$

n_i is the fractional abundance of isotope i, $\sigma_{ik} = \sigma_{i\ell}$ is the low-energy collision cross section between atoms of type i and type k, and γ_{ik} is a function of the atomic masses:

$$\gamma_{ik} = \frac{4 M_i M_k}{(M_i + M_k)^2} . \tag{4}$$

The sums are taken over all target atomic species, but k and ℓ refer only to isotopes of a single chemical element.

We emphasize that (2) applies only to the material actually sputtered away from the target, and not to the composition of the target surface

---

*This expression for $\delta_{k,\ell}$ is the one given in Watson [1980]. It differs slightly from that found in Watson and Haff [1980], although numerical values are similar in the two cases. For equal cross sections, the two expressions are identical.

subsequent to sputtering. Modification of the surface composition can be described by models which incorporate both preferential sputtering effects and subsurface diffusion processes, but such a project is beyond the scope of the work discussed here. The abundance factors n_i appearing in (2) refer to the instantaneous atomic abundances. In general these are not constant in time if $\delta \neq 0$, and thus $\delta = \delta(t)$. The results which are reported here, therefore, refer only to low dose experiments where a limited amount of material is sputtered from the sample.

To illustrate the results one would expect if fractionation occurs according to (2), we first specialize to several idealized cases. Consider a target composed of a single element, which in turn is composed of only two isotopic species, 1 and 2. The total cross sections σ_{ij} are all equal to a common value, hence

$$\delta_{1,2} = \frac{n_1 + n_2 \gamma_{12}}{n_1 \gamma_{12} + n_2} - 1 . \tag{5}$$

We let the masses be M_1 and $M_2 = M_1 + \Delta M$ for species 1 and 2 respectively, and furthermore define $\Delta M/M_1 = \epsilon$. To illustrate the fractionation behavior for small mass differences we take $\epsilon \ll 1$. Then $\gamma_{12} \approx 1 - \frac{1}{4}\epsilon^2$

$$\delta_{1,2} \approx \tfrac{1}{4}\epsilon^2 (n_1 - n_2) . \tag{6}$$

For such a two component system, the sign of the fractionation depends upon the abundance factors n_i, and not upon the mass values. Thus if $n_1 > n_2$ in the surface layer, $\delta_{12} > 0$ and species 1 is sputtered preferentially. Moreover, the fractionation effect is quadratic in the mass difference ϵ. For a mass increment of $\epsilon = 0.1$, (6) gives a maximum limiting value of 2.5 $^o/oo$ for the magnitude of the fractionation effect (see Fig. 1).

The expression given by (2), and hence the result (6), arise from a detailed solution of the transport equation describing energy sharing amongst recoiling atoms [Watson, 1980, Watson and Haff, 1980]. A source of particles is created by primary collisions between the incident ion and a target atom. These recoiling atoms are typically of very low energy, and interact much in the manner of hard spheres. For projectiles in the energy range of a few keV to a few hundred keV, a description of the sputtering process based upon such a picture [Sigmund, 1969] is well-established. Absolute sputtering yields (number of atoms ejected per incident ion) of many materials can be computed to an accuracy within a factor of two or three, and, more importantly, the dependence of the sputtering yield on incident ion energy, mass, and charge can be reproduced adequately by the cascade theory, for a wide variation in the parameters. Furthermore, the predicted E^{-2} dependence of the yield on the energy of the sputtered particle has been independently verified by several investigators [Thompson, 1968; Weller and Tombrello, 1978].

These calculations have in each case been performed for a uniform distribution of scattering centers. In an actual sputtering experiment, however, the distribution of atoms fills only a half-space. The actual calculations are thus perturbation theory calculations, with the target surface introduced only at the final step as the boundary across which the sputtering flux should be taken. Sequential collision events such as shown in Fig. 2 are included in the calculation, but cannot physically occur in the true target since the collision point is outside the target surface. Watson [1980] and Watson and Haff [1980] made an attempt to include effects introduced by the presence of a surface in a less rigorous way. They postulated that the atoms comprising the extreme outer surface layer of the

target cannot participate fully in the recoil cascade, primarily because the geometry makes it difficult for them to transfer energy to subsequent atoms after they themselves have been struck. Sputtered particles are then imagined to derive from this passive surface layer as it absorbs energy from recoiling atoms deeper in the target. It is this model, which attempts to take account of the effects of a non-uniform (i.e., half-space) distribution of target atoms, that leads to the expression (2) for the fractionation.

The "surface-flux" model was adopted because the non-stoichiometric emission of isotope species expected from the bulk recoil flux alone was found to be much smaller than indicated by experiment. Thus Russell et al. [1980] found $\delta(^{44}Ca:^{40}Ca)$ for material sputtered from a plagioclase target to be on the order of $\sim -20\,^{o}/oo$, while predictions based on non-stoichiometries in the bulk recoil flux indicated values no less than $-1\,^{o}/oo$ [Watson and Haff, 1980]. On the other hand, the surface-flux model is in adequate agreement with the data of Russell et al. [1980] for Ca fractionation in plagioclase and in fluorite. However, the peculiar fractionation patterns inherent in the model, as shown clearly by (6) which predicts (a) that the value and even the sign of δ depend upon the abundance factors of the target components and (b) that it is possible for the fractionation pattern to contain no linear term in the mass increment, have not yet been adequately tested experimentally. In the subsequent discussion we will clarify the physics behind the fractionation mechanism at issue here and suggest some further experiments designed explicitly to test the model.

We continue for a moment our discussion of a two component medium. According to Watson and Haff [1980], the bulk flux of recoiling atoms is very nearly stoichiometric (except for extreme differences in target atom masses, or for the very highest energy particles which, however, constitute only a small

portion of the total flux). This flux has an energy dependence of the form An_i/E^2, for species i, where A is a constant. For simplicity, imagine head-on collisions of these bulk-flux components with stationary surface atoms. The surface flux of type-1 atoms is then

$$dG_1 \propto n_1 \gamma_{11} A \frac{n_1}{E^2} dE + n_1 \gamma_{12} A \frac{n_2}{E^2} dE \ , \tag{7}$$

where the first term describes atoms of type-1 ejected by collision with atoms of type-1, and the second term describes atoms of type-1 ejected by collision with atoms of type-2. Equation (7) leads to the partial sputtering yields

$$dS_1 \propto n_1 \ (n_1 + \gamma_{12} \ n_2) \ dE/E^2 \tag{8}$$

and similarly

$$dS_2 \propto n_2 \ (n_2 + \gamma_{21} \ n_1) \ dE/E^2 \ . \tag{9}$$

The fractionation of the sputtered material with respect to the bulk is therefore

$$\delta_{1,2} = \frac{\int dS_1/\int dS_2}{n_1/n_2} - 1 \ , \tag{10}$$

which reduces to (5) upon substition from (8) and (9). The γ-factors in (7) come from the kinematic limits on the maximum amount of energy which can be transferred in an elastic collision. The source of the fractionation in this model is therefore seen to arise from the energy transfer mismatch between the surface species and the bulk recoil flux; i.e., it is easier to transfer energy to a similar mass in a collision than to a much different mass. The effect is larger in the surface layer than internally because of the fact that surface atoms are allowed to interact with the cascade in one step only: there is no opportunity for the effect to be averaged away over

many collisions. Equations similar to (10) and (5), and their generalization to polyatomic media, were derived by Watson [1980] and Watson and Haff [1980] without the simplifying assumption of head-on collisions used here. In the general case in which different chemical species are present in the target, the relative total collision cross sections which describe scattering of the various distinct pairs of atoms also appear in the expression for δ, as in (2).

These remarks apply to isotopic components of a single element. If more than one chemical species is present, fractionation of one chemical species from another will in general occur, but its magnitude is determined more by details of the target chemistry than the atomic masses and abundances. However, expression (2) for the fractionation applies to any target, regardless of its chemical composition, as long as it is only the fractionation amongst isotopic components of a single chemical element that is desired. Moreover, since members of any isotopic suite are ejected from the surface by means of collisions with all the atomic species in the target, it is clear that the fractionation pattern for these isotopes can depend strongly on the mass of each kind of target atom. It is this feature which we feel will provide the most convincing test of the validity of the fractionation model described here.

As an illustration of the effect of this "background" mass M_3 upon the fractionation pattern of a particular pair of isotopes 1 and 2, with masses M_1 and M_2 ($M_1 < M_2$, say), we consider a target composed principally of type-3 background atoms, with abundance n_3, but which contains a small proportion of the isotopic species 1 and 2 so that $n_1 + n_2 \ll n_3$. Type-3 atoms need not be isotopes of the same element as type-1 and type-2 atoms. The last inequality is not necessary for analysis but it leads to a clear picture

of the fractionation process. Essentially all atoms which are ejected will arise from collisions with type-3 atoms. Thus when $M_3 < M_1$, we expect species 1 to be preferentially sputtered, so that $\delta_{2,1} < 0$, but if $M_2 < M_3$, then $\delta_{2,1} > 0$. For the case $M_1 < M_3 < M_2$, the fractionation will be small, and it will vanish for some value of M_3 in this range. For this case we find from (2)

$$\delta_{2,1} \approx \frac{\gamma_{23}}{\gamma_{13}} - 1 , \tag{11}$$

since the cross sections σ_{23} and σ_{13} are equal. The fractionation in this case is independent of the abundances of the isotopes in question, as long as they are much less than unity. If $M_2 = M_1 + \Delta M$, and $\epsilon \equiv \Delta M/M_1$, then for $\epsilon \ll 1$,

$$\delta_{2,1} \approx -\epsilon \left(\frac{1 - M_3/M_1}{1 + M_3/M_1} \right) , \tag{12}$$

so that the fractionation is linear, with $-\epsilon \leq \delta_{2,1} \leq \epsilon$. Figure 3 shows $\delta_{2,1}$ as a function of M_3 for the particular choice $\epsilon = 0.1$, $M_1 = 40$ (and $M_2 = 44$). Also shown is $\delta_{2,1}$ evaluated according to (11), so that an expansion in powers of ϵ is avoided. The two curves differ significantly in the region $M_3 \approx M_1$, but they both illustrate the fact that the magnitude and sign of $\delta_{2,1}$ can be drastically affected by the choice of the chemical matrix in which the isotopic species of interest are imbedded. If for simplicity we take n_1, n_2, and n_3 to refer to isotopes of a single element, then in the special (but unlikely) case $n_1 = n_2 = n_3 = 1/3$ we find $\delta_{2,1} = \frac{1}{6}\epsilon^2$ and $\delta_{3,1} = 0$ for $M_2 = M_1 + 1$ and $M_3 = M_1 + 2$ with $\epsilon = 1/M_1 \ll 1$. Here the middle-mass isotope M_2 is better coupled to the underlying recoil cascade than either of the end members.

Although, with the exception of special cases (see (6) and the above paragraph), δ is proportional to the mass increment ϵ for small ϵ, if this quantity is not small, then δ will depend upon the increment in a more complicated way. We do not need to appeal to an expansion in ϵ to see this effect, since, within the model (2) is exact. Figure 4 gives an illustration of nonlinearities in the fractionation, due to violation of the condition $\epsilon \ll 1$, for a pure Ca target containing the terrestrial abundances of ^{40}Ca, ^{42}Ca, ^{43}Ca, ^{44}Ca, ^{46}Ca, and ^{48}Ca. The curve was calculated from (2). The δ-values with respect to ^{40}Ca are all negative since the dominant abundance of ^{40}Ca leads to preferential ejection of the lighter isotopes.

We turn now to more interesting targets, taking as a first example SiO_2. Because for the light elements stable light isotopes are generally more abundant than heavier isotopes, we would expect for a pure Si target (n_{28} = 0.9217, n_{29} = 0.0471, n_{30} = 0.0312) that $\delta_{29,28}$ and $\delta_{30,28}$ would be negative, while for a pure (solid) O target (n_{16} = 0.99759, n_{17} = 0.00037, n_{18} = 0.00204) $\delta_{17,16}$ and $\delta_{18,16}$ would also be negative. However, for the SiO_2 target, the qualitative conclusions reached for the sign of the δ-values above are no longer all necessarily true. First, although the addition of O to a Si target would tend to make the $\delta_{29,28}$ and $\delta_{30,28}$ values even more negative, the addition of Si to an O target would have the opposite effect on $\delta_{17,16}$ and $\delta_{18,16}$, and could even make them positive. There is the additional complication of the cross-section values to be used [see (3)]. When two or more chemically distinct species are present in the target with non-negligible abundances, the total low-energy scattering cross sections help to determine the fractionation values. The σ_{ij} enter the calculation because the collision probabilities determining the coupling of the surface layer to the bulk depend on the product of abundance times cross section.

Because of the structure of (3), one of these cross sections may be chosen arbitrarily, i.e., we are interested in the relative, not absolute, sputtering rates. Consequently, the fractionation values depend only upon the ratios of cross sections, and not on their magnitudes. When a target is composed of isotopes of one element only, or where collisions between such isotopes and one other distinct element are the only collisions which are important, then the ratios of all relevant cross sections become unity, as is the case in the above examples, and δ then depends on the masses and abundances alone.

To begin with, we illustrate the fractionation expected for both Si and O in SiO_2, with the values (taken from a Born-Mayer model of the atom) $\sigma_{Si \to Si}$ (= $\sigma_{28,28}$ = $\sigma_{28,29}$, etc.) = 5.91 $\mathring{A}^2$, $\sigma_{Si \to O}$ (= $\sigma_{28,16}$ = $\sigma_{28,17}$ = $\sigma_{29,16}$, etc.) = 5.14 $\mathring{A}^2$, and $\sigma_{O \to O}$ = 4.43 $\mathring{A}^2$. We find from (2)

$$\delta_{17,16} = +4.9\ ^{o}/oo$$

and

$$\delta_{18,16} = +8.0\ ^{o}/oo,$$

so that the deviation from linearity is 1.8 $^{o}/oo$. The Si fractionation values are

$$\delta_{29,28} = -6.4\ ^{o}/oo$$

and

$$\delta_{30,28} = -13.0\ ^{o}/oo,$$

which is essentially a linear relationship. The important point though is that the trend of the fractionation corresponds to preferential emission of heavy isotopes for one chemical element (O), and to preferential emission of light isotopes for another (Si).

The above values are dependent upon the cross sections for scattering of Si and O atoms. To get an idea of the sensitivity of δ to the choice of cross section, we arbitrarily interchange the Si → Si scattering cross section with the O → O scattering cross section in the evaluation of δ, i.e., $\sigma_{Si \to Si} \to 4.43\ \mathring{A}^2$, $\sigma_{O \to O} \to 5.91\ A^2$, but $\sigma_{Si \to O} = 5.14\ A^2$ as before.

Then

$$\delta_{17,16} = 3.9\ ^{o}/oo$$

and

$$\delta_{18,16} = 5.9\ ^{o}/oo,$$

with roughly the same amount of non-linearity as above, while

$$\delta_{29,28} \approx -6.9\ ^{o}/oo$$

and

$$\delta_{30,28} = -14.1\ ^{o}/oo,$$

still almost linear. Finally, in the case that all cross sections are set equal to each other, we find

$$\delta_{17,16} = 4.1\ ^{o}/oo,$$

$$\delta_{18,16} = 6.4\ ^{o}/oo,$$

$$\delta_{29,28} = -6.5\ ^{o}/oo,$$

and

$$\delta_{30,28} = -13.2\ ^{o}/oo.$$

Figure 5 summarizes the fractionation patterns for these three choices of the cross sections.

The dependence of δ upon the (generally not well-known) collision cross sections is a fact one must live with. It makes a reliable calculation

of expected δ-values more difficult. Still, the patterns illustrated in Fig. 5 are relatively stable against variations in the σ_{ij}. One reason is that only the relative values of the cross section are required in (3).

In order to illustrate the application of the above results to particular targets, we give some examples of predictions based upon (2) as applied to selected high temperature condensate minerals. Mineral targets were chosen for several reasons. The most complete characterization of isotopic fractionation effects induced by sputtering was recently carried out on plagioclase and fluorite targets [Russell et al., 1980]. The present model was developed in part to try to understand these results. In earlier work the question of isotopic fractionation of mineral components during sputtering was addressed by Switkowski et al. [1977] to try to account for the observed abundance of Si and O isotopes in lunar fines. More recently Clayton [1980] has raised the question of whether sputtering of interstellar grains could be the source of certain isotopic anomalies observed in meteoritic inclusions. In the examples illustrated below we do not endeavor to come to grips with the problem of the likeliness of sputtering as a significant isotopic fractionating agent in pre-solar system history, but it is nevertheless interesting to see how appropriate mineral phases [Grossman, 1972] would be expected to fractionate in the present model. By presenting these examples, we also gain a clearer idea of the magnitude of the effects which might be expected in an actual experimental test of the model.

Figures 6-10 show the predicted fractionation patterns for all sets of isotopes in, respectively, perovskite ($CaTiO_3$), plagioclase (anorthite) ($CaAl_2Si_2O_8$), melilite (akermanite ($Ca_2MgSi_2O_7$)), enstatite ($MgSiO_3$), and troilite (FeS). To be definite we have set all cross sections equal. The patterns exhibit several interesting features. Perhaps

most striking is the fact that the fractionation effect in one mineral looks essential the same as in any other mineral containing the same kinds of atoms. The same basic pattern is also encountered in a number of other minerals not illustrated here: corundum (Al_2O_3), magnetite (Fe_3O_4), rutile (TiO_2), eskolaite (Cr_2O_3), various spinels ($FeAl_2O_4$, $ZnAl_2O_4$, $MnAl_2O_4$, $MgAl_2O_4$), gehlenite ($Ca_2Al_2SiO_7$), hibonite ($CaAl_{12}O_{19}$), fluorite (CaF_2), albite ($NaAlSi_3O_8$), diopside ($CaMgSi_2O_6$), and forsterite (Mg_2SiO_4). In each case O is fractionated to a level of roughly 4-6 $^o/oo$ per mass unit, with a slight ($\sim$ 1.8 $^o/oo$), but remarkably constant, non-linearity, to be discussed below. The O curves correspond to positive fractionation, and the reason is the same as for the O component of quartz, Fig. 5. In each mineral ^{16}O is the lightest component, and the coupling to the high mass components leads to preferential emission of the heavy isotopes. The effect is not a strong function of the mass of the heavy atoms, as long as they are reasonably abundant. In the O-containing minerals illustrated above, O accounts for, to within a few percentage points, 60% of all atoms by number, while the heavier atoms, usually some combination of Al, Mg, Si, and Ca, make up the remaining 40%. Thus O fractionation does not vary much from one mineral to the next. For similar reasons, the heavier components of the mineral are in each case negatively fractionated, i.e., the lighter isotopes are sputtered preferentially.

The same kind of results are predicted for the non-oxygen containing mineral troilite (FeS). S is positively fractionated and Fe negatively fractionated, in both cases at the level of a few parts per thousand (ppt) per unit mass.

These seem to be the two hallmarks of sputter-induced isotopic fractionation in many minerals: (1) all isotopes are fractionated at the level

of a few ppt per unit mass, independently of the precise mineralogy of the target, and (2) sputtered O is isotopically heavy with respect to the O in the target, while heavier sputtered elements (Mg, Si, Ca, Ti) are isotopically light. The magnitudes of the fractionations predicted are large compared to the precision of the most careful mass spectrometric analyses (~ 0.1 ‰ [Lee, 1979]). The fact that sputtering of isotopes of the light and heavy elemental components of a given target is predicted to produce fractionations of different sign sharply distinguishes the kind of process described here from mechanisms based on thermal or diffusive kinetics, which can also lead to isotopic fractionation. Fractionation due to mechanisms such as these must be either positive or negative, but not both, for a given set of processed isotopes. The "mixed" positive and negative fractionation patterns produced in this model would be suggestive signatures for the origin of any material which exhibited them.

Some of the illustrated fractionation curves exhibit, in addition, definite non-linearities. The most regular and for the most part the largest of these is shown by the O series. In every case studied, ^{18}O is less abundant in the sputtered material than a linear relation based on the $\delta(17,16)$ value would suggest. Alternatively, based on the $\delta(18,16)$ value, we could say that the ^{17}O abundance is enhanced. Our procedure has been to compare all δ-values predicted according to (2) with a straight-line value obtained by passing a line through the origin and through the δ-value for the lightest pair $(M + \Delta, M)$ of stable isotopes. The upper panels in Figs. 8-10 show the non-linearities calculated by this scheme,

$$\xi_{M+i} \equiv i\ \delta(M+\Delta,M) - \delta(M+i,M)\ . \qquad (15)$$

The ξ-values for $\delta(18,16)$ are confined to the narrow range + 1.8 to + 1.9 ‰ and are essentially independent of the mineralogical matrix. Small non-

linear features also appear in some of the heavier isotopic series, but they are neither so regular nor generally so large as those found for O.

Before pursuing the possibilities inherent in a mechanism which can lead to anomalous isotopic patterns, however, we need to establish the validity of the model proposed here, and this can be done only by appeal to appropriate experiments. The present model arose out of the Ca fractionation data of Russell et al. [1980]. Watson and Haff [1980] found it necessary to invoke the surface flux model in order to obtain fractionation values of the magnitude required. But the model did not predict the experimental results; it can be said only to be consistent with them. However, the predicted positive-negative fractionation pattern illustrated in the above figure provides the kind of yes-no test that can give substantial support for or evidence against the proposed sputtering mechanism.

A test that seems to have merit involves measuring isotope ratios from the same chemical element in two different targets. The "background" masses of the auxiliary partners would be different in the two cases, and chosen to yield an expected positive fractionation of the isotopes of the given element in one case and a negative fractionation in the other. Because experience has already been gained in the measurement of fractionation of Ca-containing minerals under sputtering conditions [Russell et al., 1980], we examine predictions of (2) for two possible Ca-containing targets.

Figure 11 shows expected fractionations for fluorite, CaF_2, and for CaI_2. The elements F and I are each composed of a single stable isotope with mass 19 and 127, respectively, and these two masses bracket the range of the Ca isotopes. The Ca sputtered from CaF_2 is predicted to be strongly fractionated in a negative sense, and the Ca sputtered from CaI_2 in a positive sense. The magnitudes of the δ-values are large, ranging from ~ 10 ‰ to ~ 50 ‰.

Moreover, especially in the case of CaI_2, the non-linearities are also large, the maximum ξ-value exceeding 7 $^{o}/oo$. The direction of the non-linearity is the same (positive) for both CaF_2 and CaI_2. This is also the case for the Ca-metal fractionation curve illustrated in Fig. 4. A positive ξ-value for a given isotope means that the isotope is more depleted in the sputtered material than a straight-line law based on the two lightest isotopes would suggest. Thus for CaI_2, the enrichment of heavy isotopes is less than the value of $\delta(42,40)$ suggests, and for CaF_2, the depletion of heavy isotopes exceeds a prediction based upon $\delta(42,40)$. This target pair could provide, then, an economical test of the sputtering model proposed here, since both the positive-negative fractionation feature as well as the non-linearity characteristic can be investigated at the same time.

We conclude the presentation of this sputter-induced fractionation process by discussing some of the qualifications and difficulties which attend it. First, it must be emphasized again that the δ-fractionation values apply strictly to the material which is sputtered away in the initial stages of bombardment, not to the surface material which is left behind. Furthermore, since δ depends upon the abundance of the various constituents at the surface [the n_i in (3)], the amount of fractionation will change as sputtering proceeds. In principle, the n_i's should be considered to be functions of time, $n_i = n_i(t)$, and therefore $\delta = \delta(t)$. The total effective δ would then be obtained by integration. Unfortunately this is a complicated and uncertain procedure. The time dependence of $n_i(t)$ depends not only on the instantaneous partial sputtering yields of the various species, but it depends also upon how the material at the extreme outer surface is mixed

with the underlying material. This mixing process [Haff and Switkowski, 1977] always accompanies ion bombardment in the region of a concentration gradient, and at the present time we are unable to treat the effect in a suitably quantitative manner. A rule of thumb which has been found useful is that preferential sputtering effects persist, at decreasing levels, until a thickness of material on the order of the range of the incident ion has been removed. For typical sputtering experiments this distance is quite small, on the order of 1700 Å in the experiments of Russell et al. [1980]. These authors found in fact that δ-values approached zero once 15-50% of the ion range had been sputtered away. The δ-values quoted in this paper refer to the material removed in the very first moments of sputtering. Subsequent sputtering can be expected to lead to a dilution of the effect, and hence to smaller effective δ-values for the sputtered material. (Clearly $\delta \to 0$ rigorously when the target has been entirely sputtered away.) For this reason the δ-values predicted here will tend to overestimate the corresponding measured quantity. Watson and Haff [1980] found that their predicted fractionation effects exceeded the measured values typically by a factor on the order of 2.

It is also important to keep in mind that the surface flux model, on which all the above results are based, is an idealized and perhaps not totally consistent treatment of the effect which the introduction of a half-space-type boundary can be expected to have an emission of particles from the surface. Thus, if the true composition of the sputtered flux contains, in addition to the surface flux, a component arising directly from the (essentially stoichiometric) internal recoil cascade, then the predicted fractionation effects will be reduced.

Nevertheless, one can pose a rather definite test of these ideas, as

exemplified by the CaF_2, CaI_2 system. A negative result in such an experiment would force a close re-examination of the surface flux model. A positive result would provide a significant stimulus to further investigations into the fractionation process. Especially interesting are problems which need to be addressed about the role of sputtering processes in space. Observed isotopic patterns in meteoritic inclusions provide important clues to the origin of the sun and planets. Since sputtering of grains by shock waves in the interstellar medium is likely to have occurred [Dwek and Scalo, 1979], we may ask how the resulting fractionations combine with those induced by nuclear reactions. The answer to such questions will depend upon the outcome of experiments designed to test fractionation theories such as presented here.

ACKNOWLEDGMENTS

PKH would like to thank Professors William A. Fowler and G. J. Wasserburg for focussing his attention on sputtering processes in mineral assemblages. Helpful comments from Professors D. S. Burnett and D. A. Papanastassiou have been incorporated in the text.

REFERENCES

Clayton, D. D., Origin of Ca Al-rich inclusions: II sputtering and collisions in the three-phase interstellar medium, submitted to Astrophys. J., 1980.

Dwek, E., and J. Scalo, Interstellar depletions and the filling factor of the hot interstellar medium, Astrophys. J. (Letters), 233, L81-L85, 1979.

Grossman, L., Condensation in the primitive solar nebula, Geochim. Cosmochim. Acta, 36, 597-619, 1972.

Haff, P. K., and Z. E. Switkowski, On the sputtering of binary compounds, Appl. Phys. Lett., 29, 549-551, 1976.

Haff, P. K., and Z. E. Switkowski, Ion-beam-induced atomic mixing, J. Appl. Phys., 48, 3383-3386, 1977.

Lee, T., New isotopic clues to solar system formation, Rev. Geophys. Space Phys., 17, 1591-1611, 1979.

Liau, Z. L., W. L. Brown, R. Homer, and J. M. Poate, Surface layer composition changes in sputtered alloys and compounds, Appl. Phys. Lett., 30, 626-628, 1977.

Russell, W. A., D. A. Papanastassiou, and T. A. Tombrello, The fractionation of calcium isotopes by sputtering, Rad. Effects, 52, 41-52, 1980.

Sigmund, P., Theory of sputtering. I. Sputtering yield of amorphous and polycrystalline targets, Phys. Rev., 184, 383-416, 1969.

Switkowski, Z. E., P. K. Haff, T. A. Tombrello, and D. S. Burnett, Mass fractionation of the lunar surface by solar wind sputtering, J. Geophys. Res., 82, 3797-3804, 1977.

Thompson, M. W., The energy spectrum of ejected atoms during the high energy sputtering of gold, Phil. Mag., 18, 377-414, 1968.

Watson, C. C., Topics in classical kinetic transport theory with applications to the sputtering and sputter-induced mass fractionation of solid surfaces and planetary atmospheres, Ph.D. thesis, Yale University, 1980.

Watson, C. C., and P. K. Haff, Sputter-induced fractionation at solid surfaces, J. Appl. Phys., 51, 691-699, 1980.

Weller, R. A., and T. A. Tombrello, Energy spectrum of sputtered uranium — a new technique, Rad. Effects, 37, 83-92, 1978.

FIGURE CAPTIONS

Fig. 1. The δ-value of (6) is plotted for a binary medium of two isotopic species M_1, M_2 with abundances n_1, n_2. The masses are related according to $M_2 = M_1 + \Delta M$, and $\epsilon = \Delta M/M_1$ is taken to have a value of 0.1.

Fig. 2. This schematic picture shows the type of unphysical collision (taking place outside the solid) which is unavoidably included in most calculations of the sputtering yield. The surface flux model attempts to partly compensate for the errors introduced in such calculations by decoupling the extreme surface layer of the target from the recoil cascade, except for collisions which actually yield a sputtered particle.

Fig. 3. This figure shows the fractionation predicted for a hypothetical target containing traces of mass 40 and 44 imbedded in a "background" matrix of atomic mass M_3. The dashed curve shows the fractionation calculated in the linear approximation (12), and the solid curve gives the exact fractionation calculated according to (2). The characteristic change over from negative to positive fractionation as a function of the background mass is clearly shown. Note that the non-linearity in the fractionation of the isotopes 40 and 44 is not given by the deviation from a straight line of the curves shown here, since only the δ-values for a single pair are represented.

Fig. 4. The curve shows the predicted fractionation in a pure Ca metal target containing terrestrial abundances of the isotopes. The deviation from linearity is due to higher order terms in the mass increment ϵ. The leading term is linear.

Fig. 5. The three curves in (a) and (b) summarize the fractionation pattern for three different choices of the relative scattering cross sections in an SiO_2 target. In (a), curve 1 corresponds to $\sigma_{O-O}/\sigma_{Si-O} = 0.86$, curve 2 corresponds to $\sigma_{O-O}/\sigma_{Si-O} = 1.16$, and curve 3 corresponds to $\sigma_{O-O}/\sigma_{Si-O} = 1.0$. In (b), curve 1 corresponds to $\sigma_{Si-Si}/\sigma_{Si-O} = 1.15$, curve 2 corresponds to $\sigma_{Si-Si}/\sigma_{Si-O} = 0.87$, and curve 3 corresponds to $\sigma_{Si-Si}/\sigma_{Si-O} = 1.0$.

Fig. 6. In (a), (b), and (c) the lower panels show the fractionation δ for O, Ca, and Ti, respectively, in perovskite, $CaTiO_3$. The upper panels in each case show the deviation from linearity as defined by (15).

Fig. 7. In (a), (b), and (c) the lower panels show the fractionation δ for O, Ca, and Si, respectively, in anorthite, $CaAl_2Si_2O_8$. The upper panels in each case show the deviation from linearity as defined by (15).

Fig. 8. In (a), (b), (c), and (d) the lower panels show the fractionation δ for O, Ca, Si, and Mg, respectively, for ackermanite, $Ca_2MgSi_2O_7$. The upper panels in each case show the deviation from linearity as defined by (15).

Fig. 9. In (a), (b), and (c) the lower panels show the fractionation δ for O, Si, and Mg, respectively, in enstatite, $MgSiO_3$. The upper panels in each case show the deviation from linearity as defined by (15).

Fig. 10. In (a) and (b) the lower panels show the fractionation δ for S and Fe, respectively, in troilite, FeS. The upper panels in each case show the deviation from linearity as defined by (15).

Fig. 11. The Ca fractionation curves for CaF_2 (bottom) and CaI_2 (top) are shown. The insets depict the deviation of these curves from a straight line through the origin and through the $\delta(42,40)$ point.

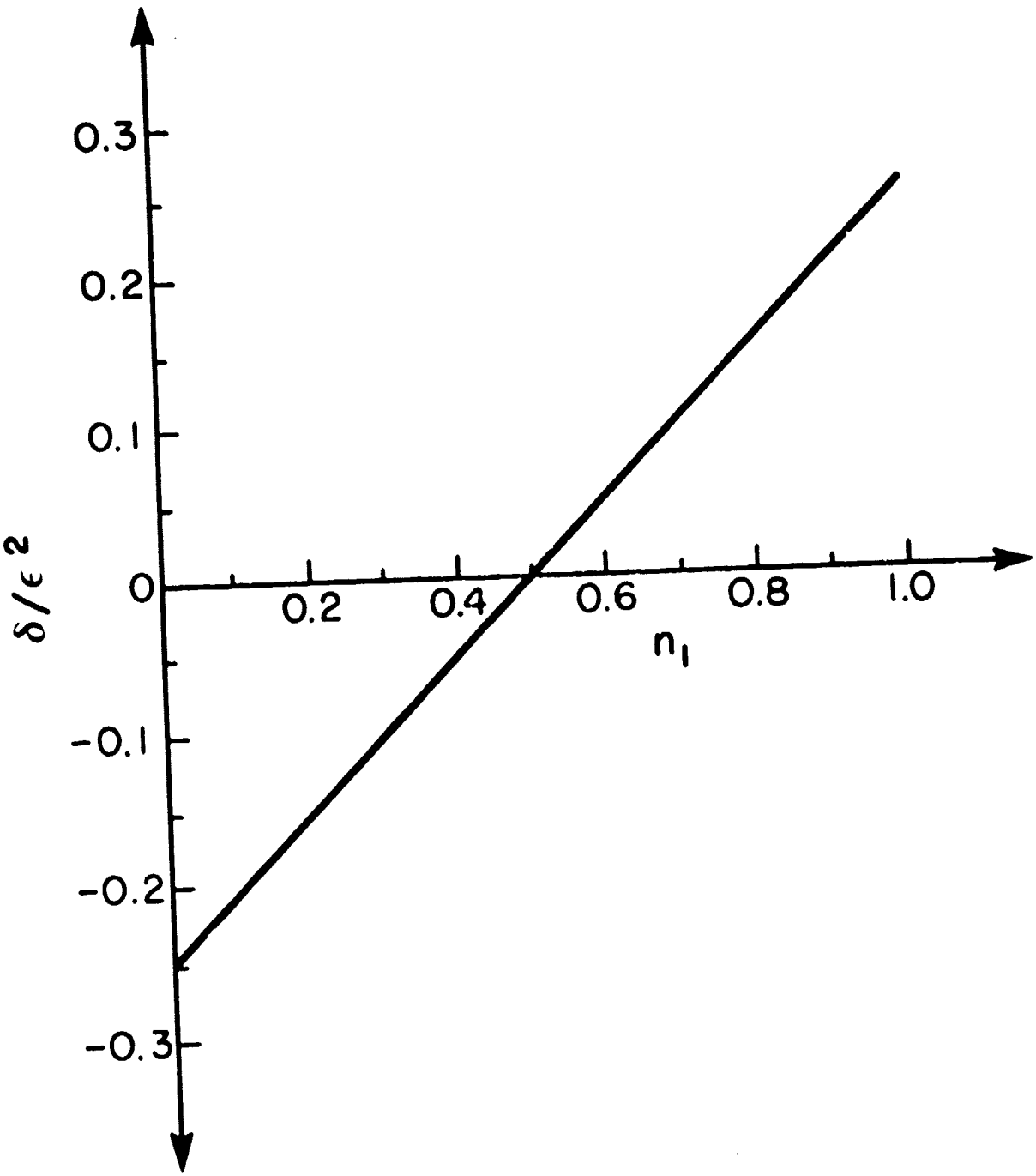

Fig. 1

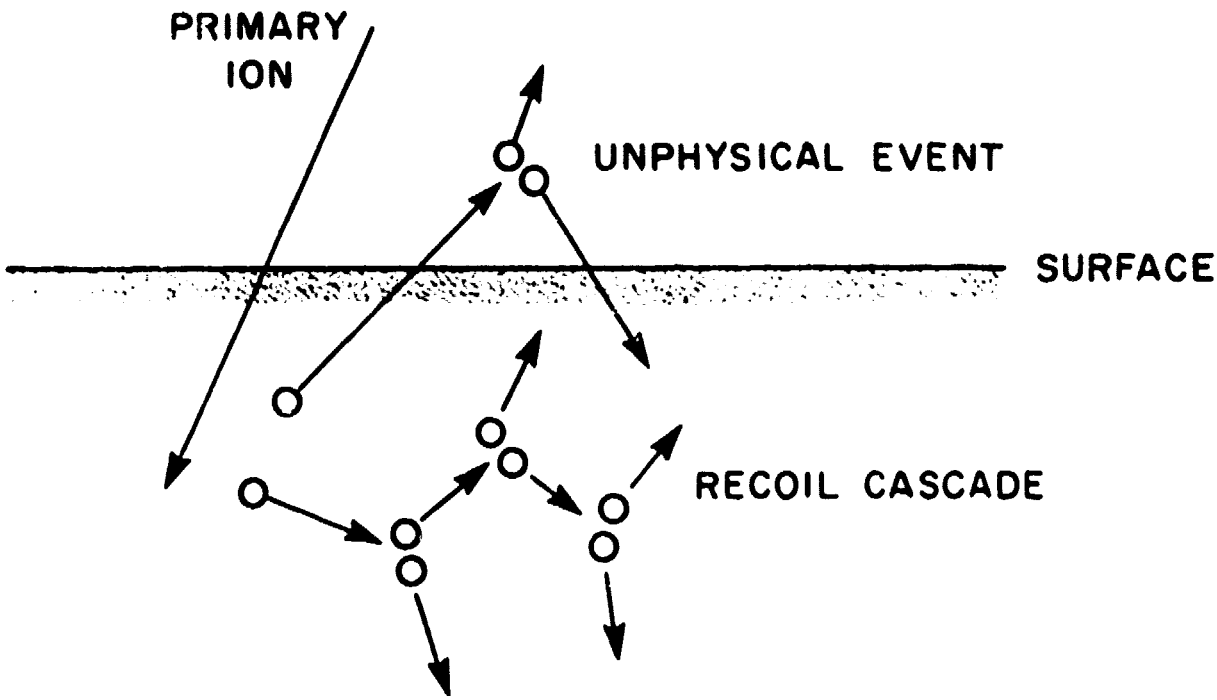

Fig. 2

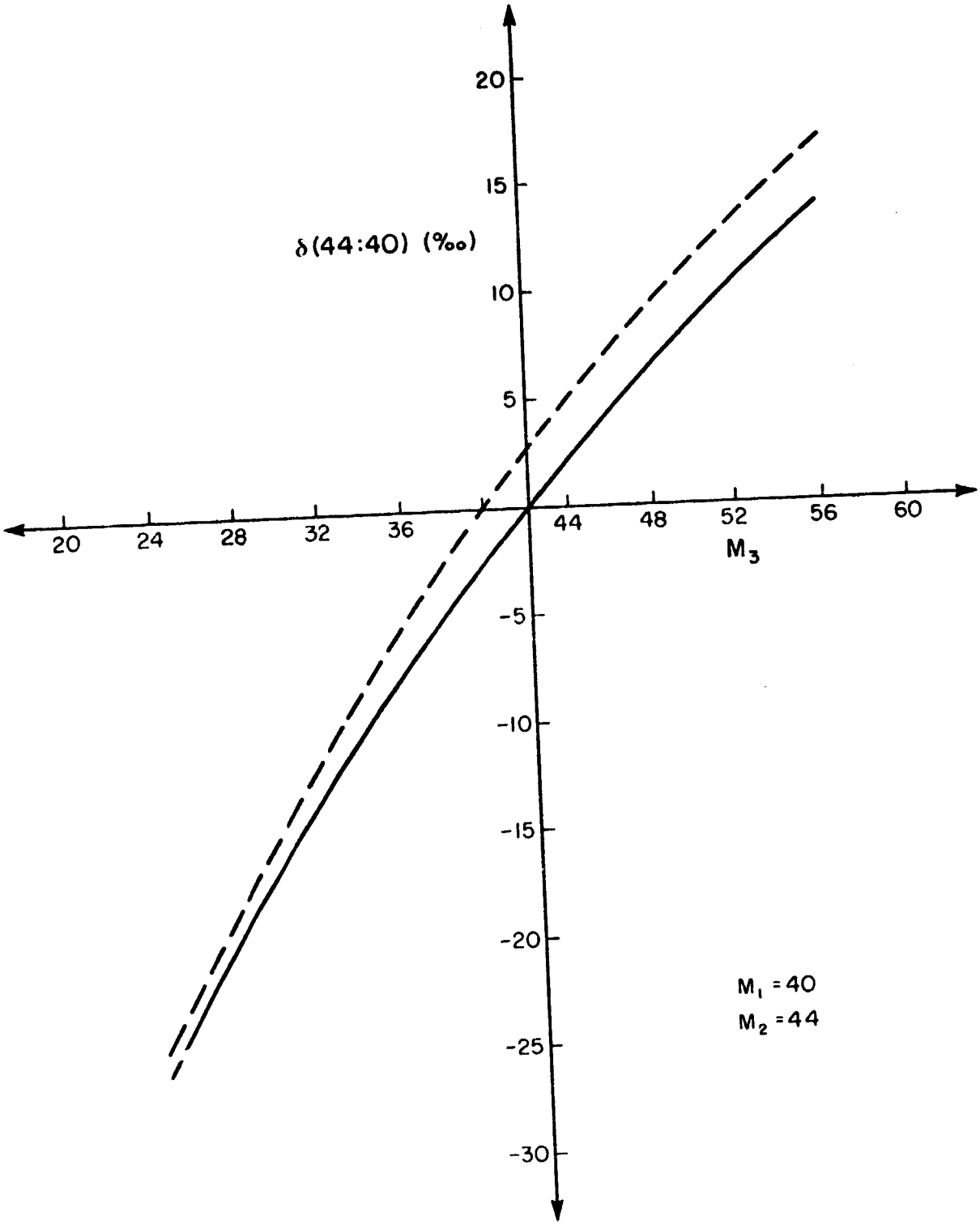
δ(44:40) (‰)
20
15
10
5
-5
-10
-15
-20
-25
-30
20
24
28
32
36
44
48
52
56
60
M3
M1 = 40
M2 = 44

Fig. 3

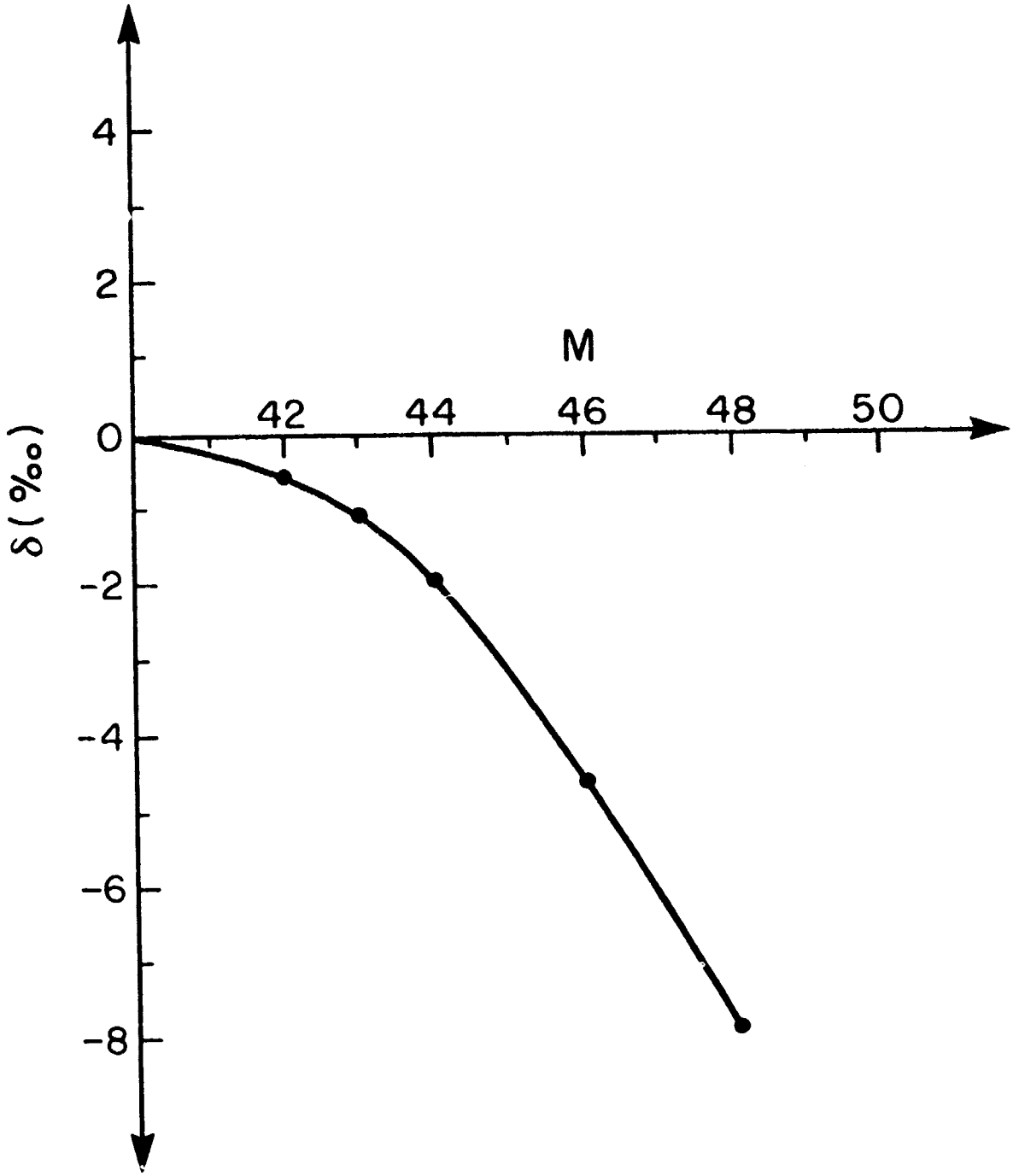

Fig. 4

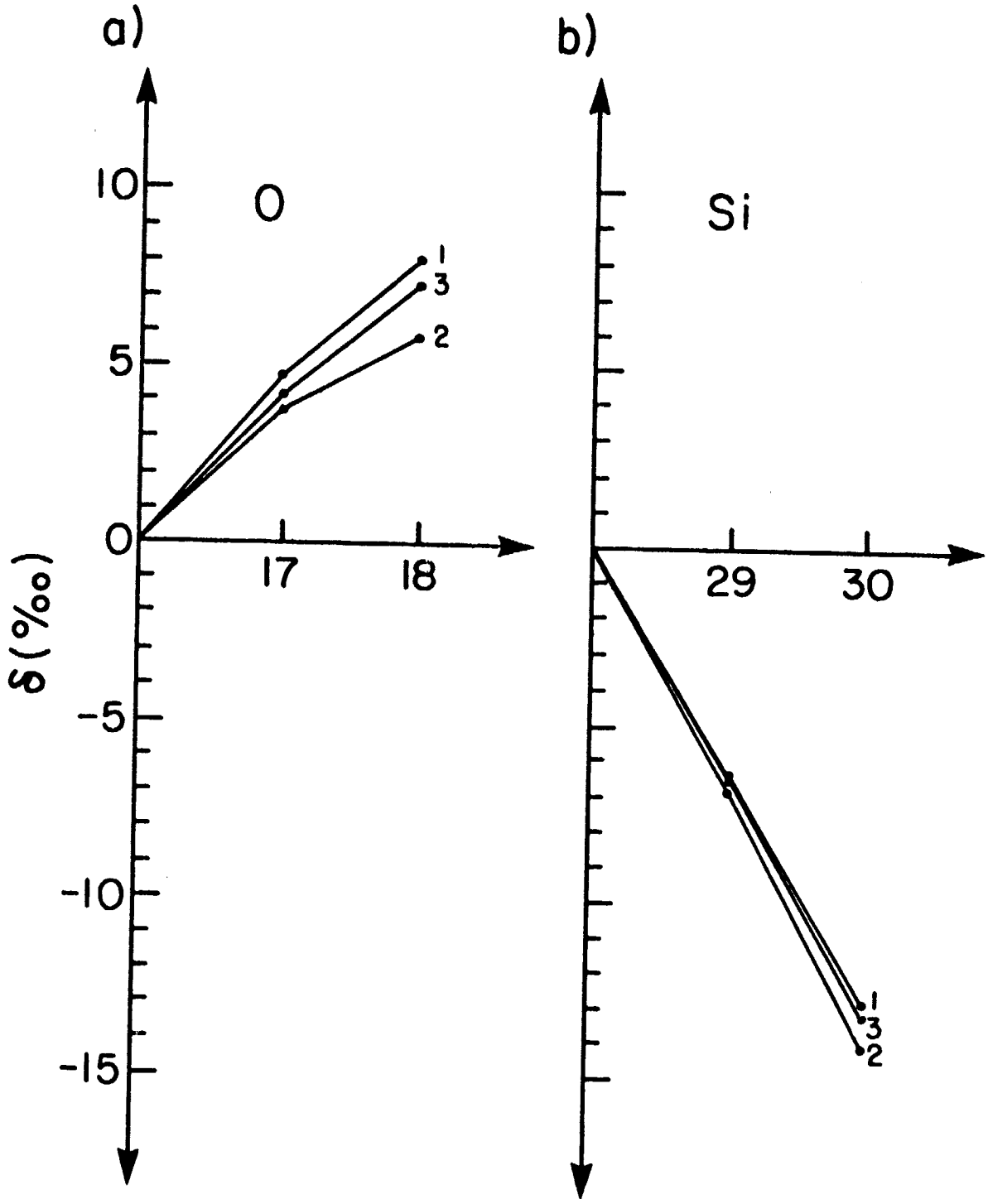

Fig. 5

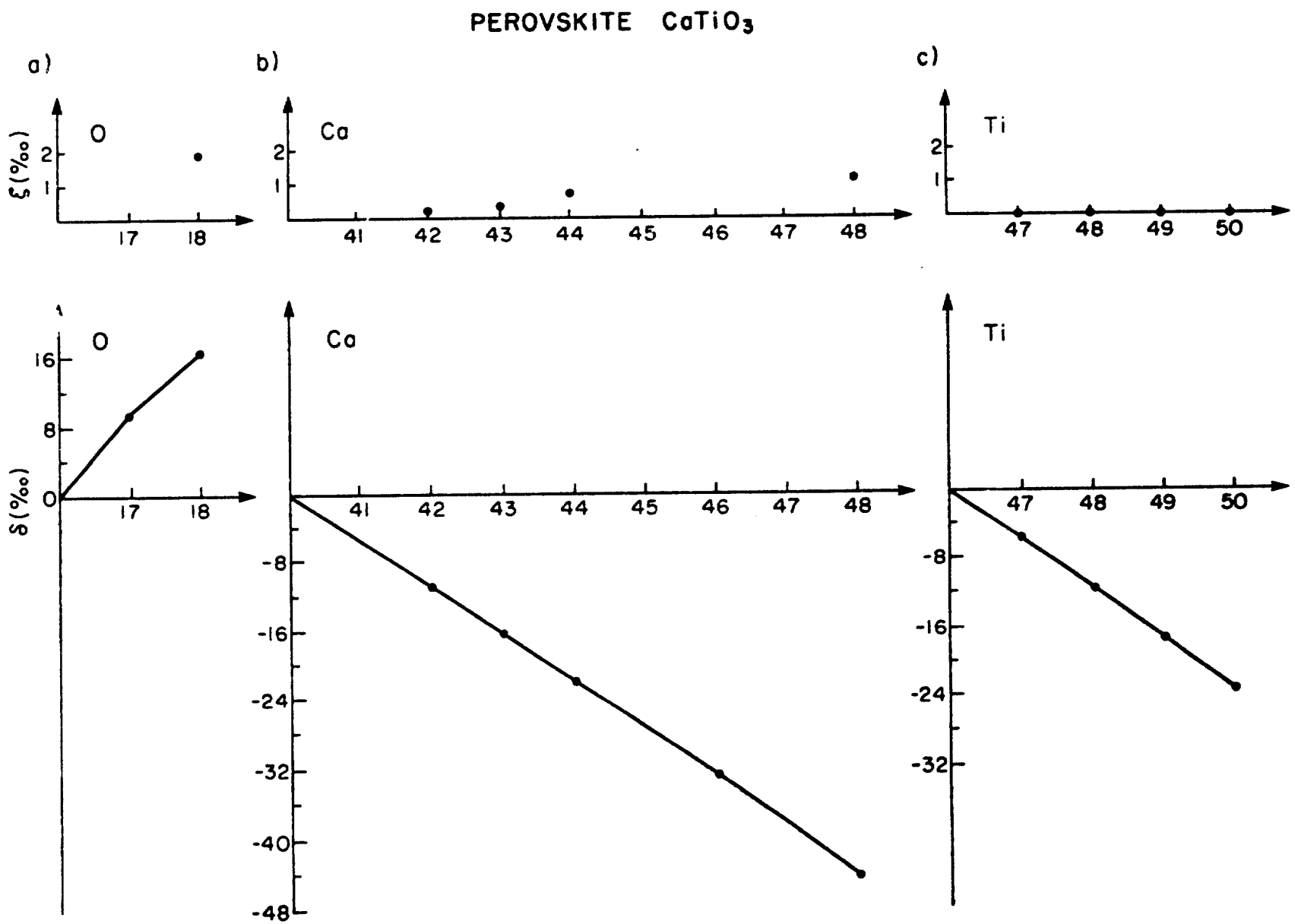
PEROVSKITE CaTiO3
a)
b)
c)
O
Ca
Ti
ξ(‰)
δ(‰)
17
18
41
42
43
44
45
46
47
48
49
50
1
2
16
8
0
-8
-16
-24
-32
-40
-48

Fig. 6

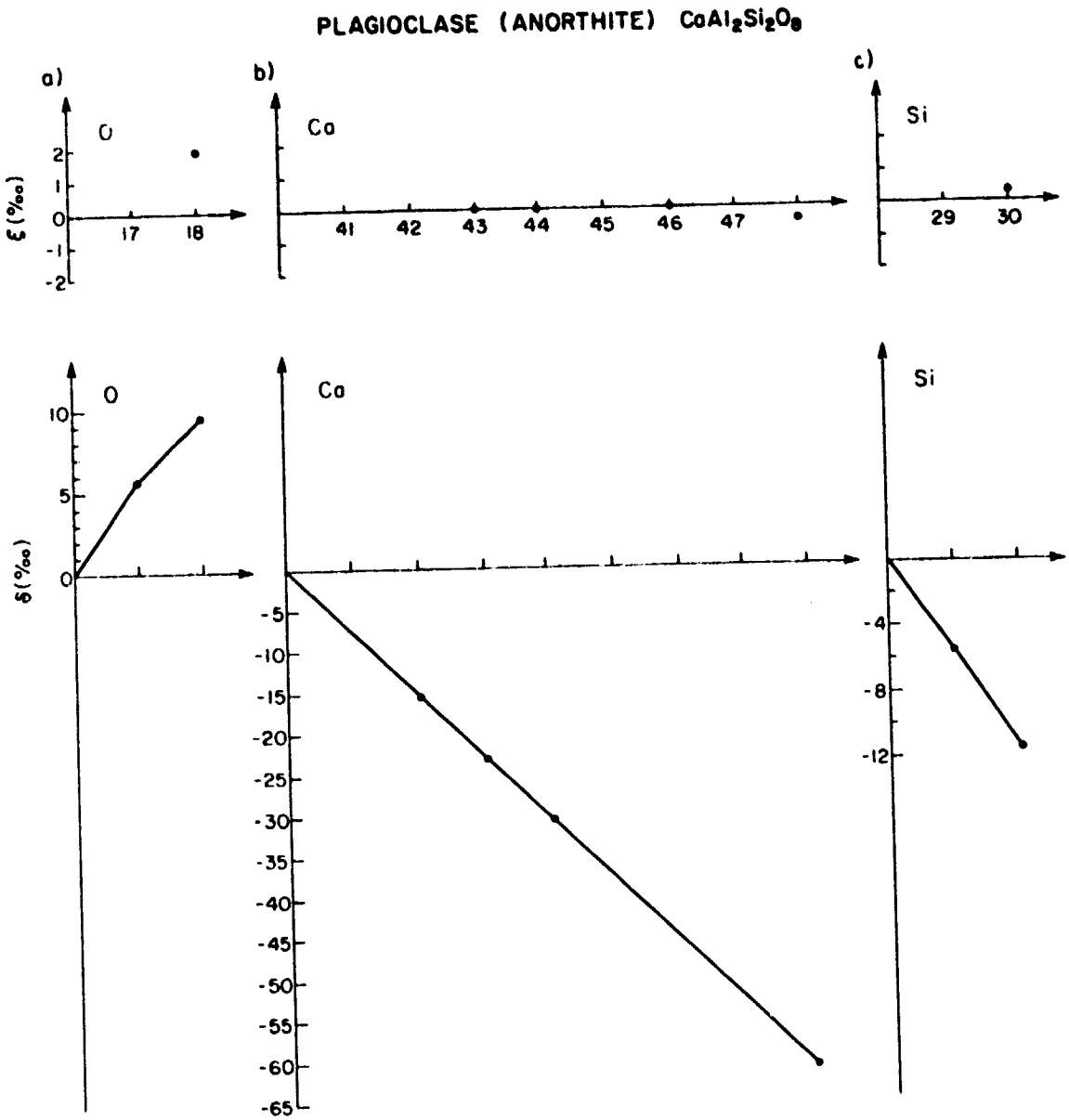
PLAGIOCLASE (ANORTHITE) $CaAl_2Si_2O_8$
a)
b)
c)
O
Ca
Si
ε (‰)
2
1
0
-1
-2
17
18
41
42
43
44
45
46
47
29
30
δ (‰)
10
5
0
-5
-10
-15
-20
-25
-30
-35
-40
-45
-50
-55
-60
-65
-4
-8
-12

Fig. 7

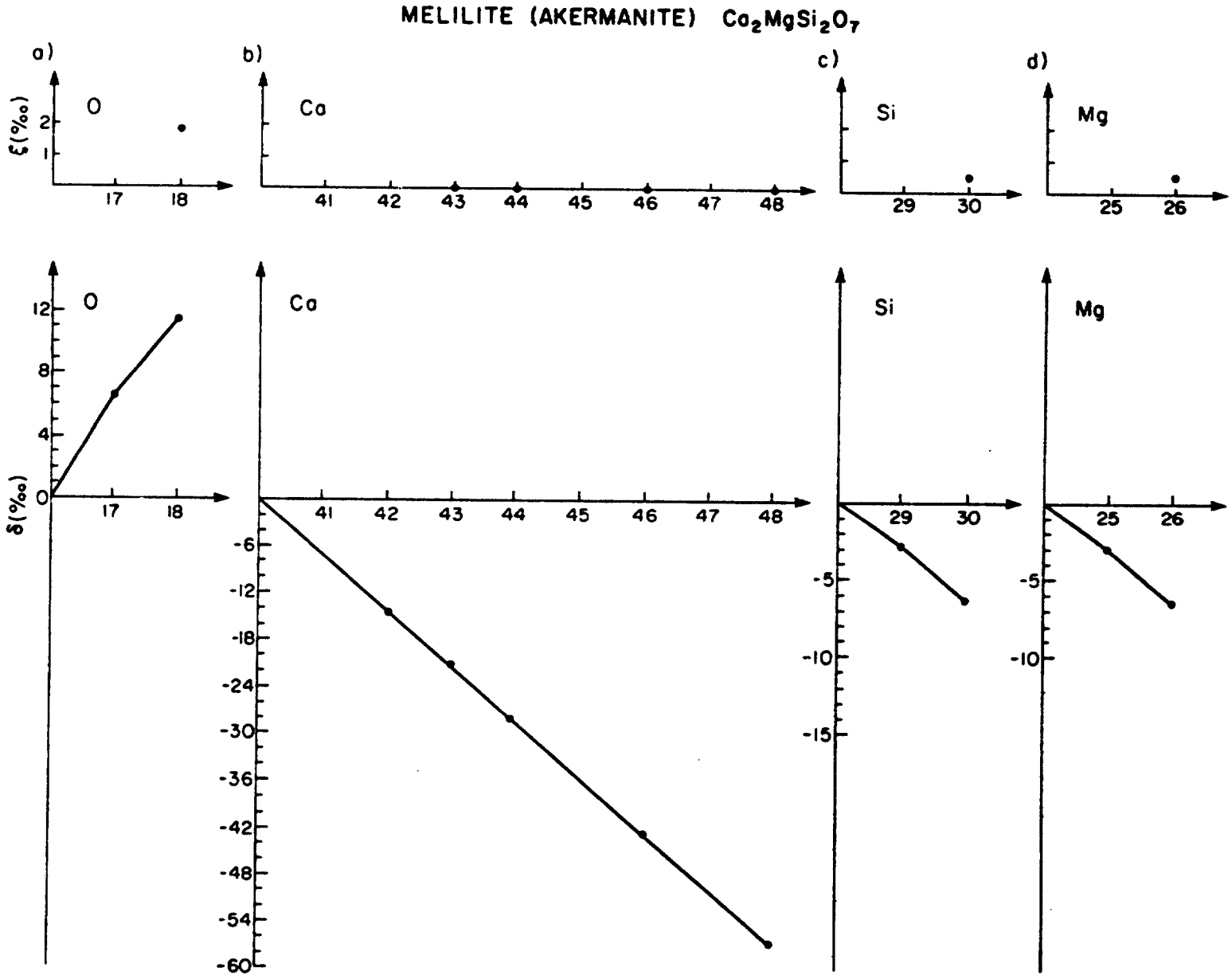
MELILITE (AKERMANITE) $Ca_2MgSi_2O_7$
a)
b)
c)
d)
O
Ca
Si
Mg
ξ(‰)
δ(‰)
17
18
41
42
43
44
45
46
47
48
29
30
25
26

Fig. 8

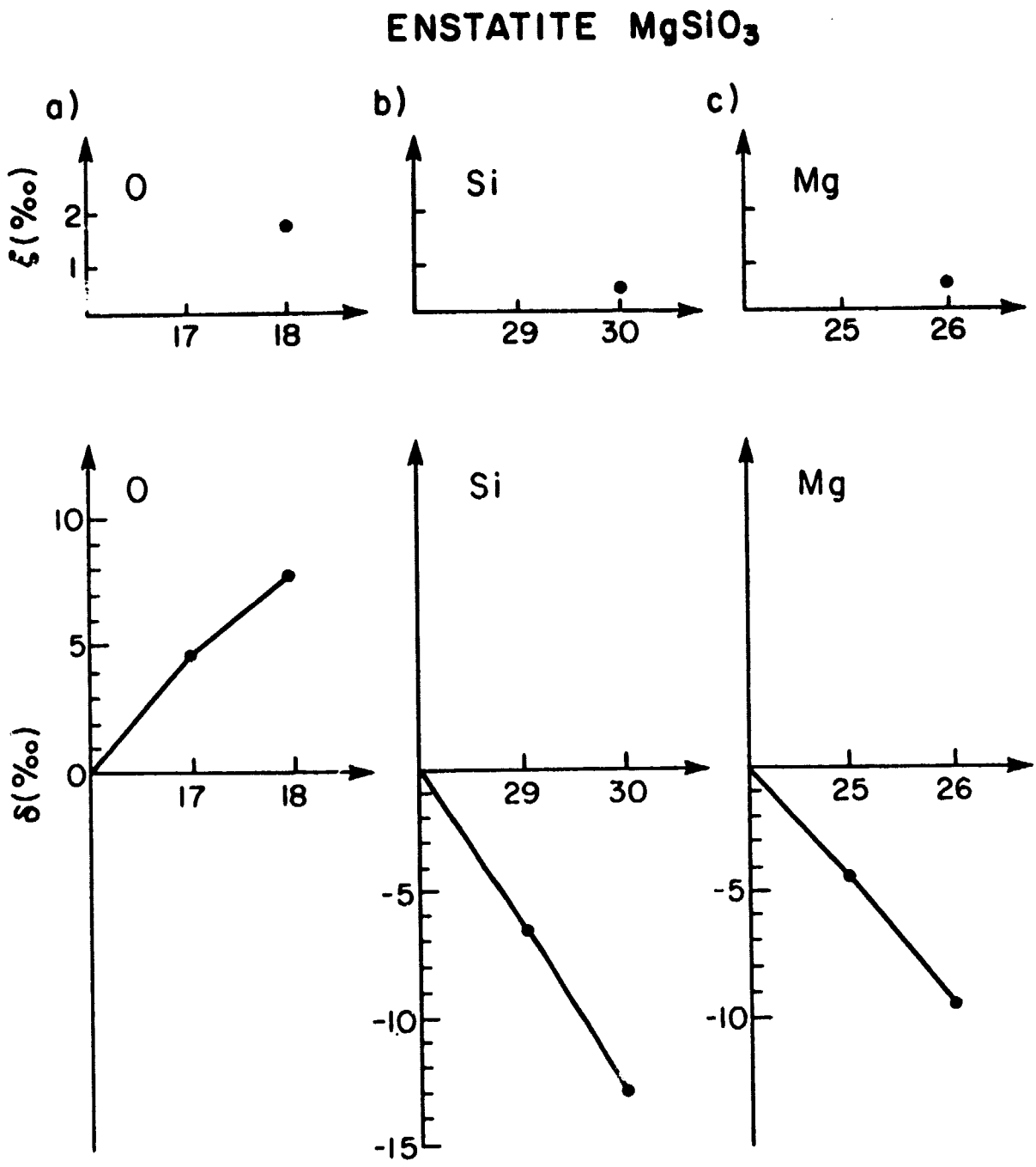
ENSTATITE MgSiO3
a)
b)
c)
O
Si
Mg
ξ(‰)
2
1
17
18
29
30
25
26
O
Si
Mg
10
5
0
δ(‰)
17
18
29
30
25
26
-5
-10
-15
-5
-10

Fig 3

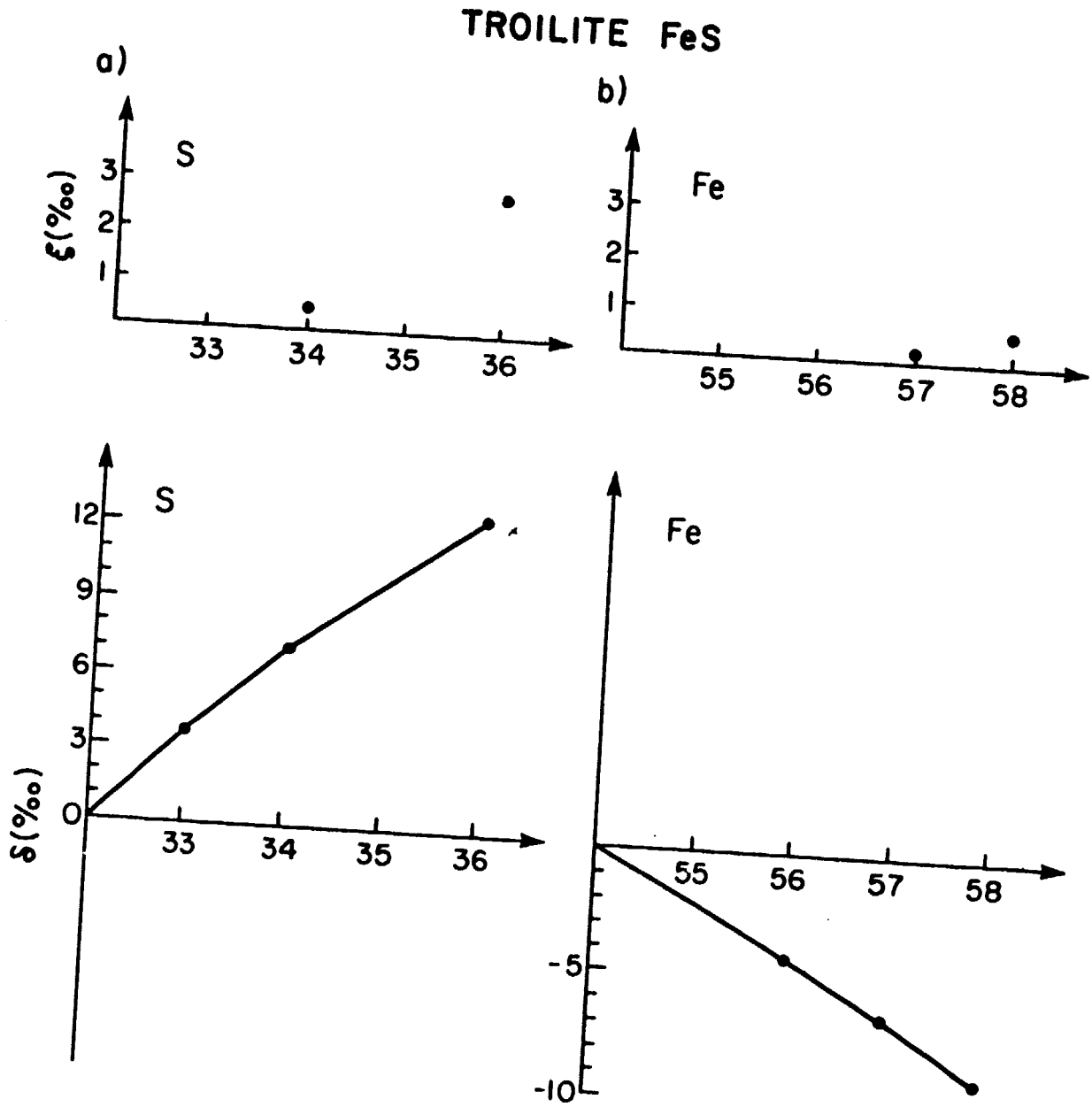
TROILITE FeS
a)
S
ξ(‰)
3
2
1
33
34
35
36
b)
Fe
3
2
1
55
56
57
58
S
12
9
6
3
0
δ(‰)
33
34
35
36
Fe
55
56
57
58
-5
-10

Fig. 10

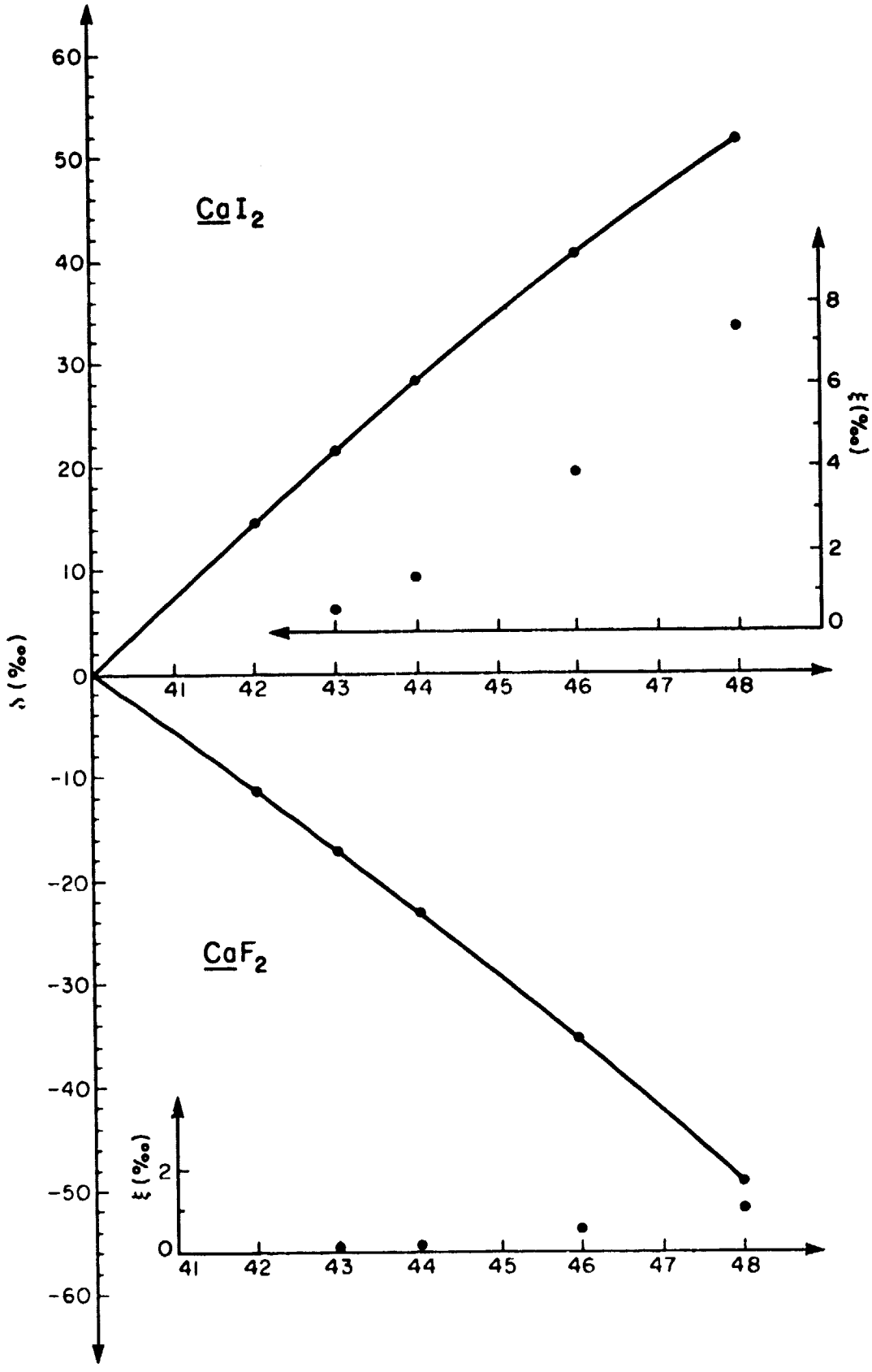
CaI2
CaF2
δ (‰)
ξ (‰)
60
50
40
30
20
10
0
-10
-20
-30
-40
-50
-60
41
42
43
44
45
46
47
48
8
6
4
2
0

Fig. 11